Inorg. Chem. **2008**, *47*, 10825−10831

$Li_{14.7}Mg_{36.8}Cu_{21.5}Ga_{66}$: An Intermetallic Representative of a Type IV Clathrate

Qisheng Lin and John D. Corbett*

Department of Chemistry, Iowa State University, Ames, Iowa 50011

Received February 20, 2008

Synthetic explorations in the quaternary Li−Mg−Cu−Ga system yield the novel intermetallic $Li_{14.7(8)}Mg_{36.8(13)}Cu_{21.5(5)}Ga_{66}$ [P$\bar{6}m2$, $Z = 1$, $a = 14.0803(4)$ Å, $c = 13.6252$ (8) Å] from within a limited composition range. This contains a unique three-dimensional anionic framework consisting of distinct interbonded Ga_{12} icosahedra, dimerized $Li@(Cu,Mg)_{10}Ga_6$ icosioctahedra, and 15-vertex $Li@(Cu,Mg)_9Ga_6$ and $Li@Cu_3Ga_{12}$ polyhedra. These polyhedral clusters are hosted by M_{20} (5^{12}), M_{24} ($5^{12}6^2$), and M_{26} ($5^{12}6^3$) (M = Li/Mg) cages, respectively. The geometries and arrangements of these cages follow those in known type IV clathrate hydrates.

Introduction

Polar intermetallics containing the elements from the groups that neighbor the Zintl border, which separates triels (group 13) and tetrels (group 14 elements), usually exhibit diverse stoichiometries, fascinating structures, novel bonding features, and specific electronic requirements.[1] Generally, Zintl phases containing the tetrels follow classic octet rules, meaning that the bonds around the tetrels originate from the atoms' s and p orbital mixings and are directional. As a result, tetrels in polar intermetallics tend to form three-dimensional anionic frameworks of 4-bonded atoms in dodecahedral-like cages (e.g., the 20-atom pentagonal dodecahedron, the 24-atom tetrakaidecahedron, the 28-atom hexakaidecahedraon, and so forth), and these often host electropositive metals, as in many examples of intermetallic clathrates.[2] On the contrary, triels do not always exhibit such directional bonding; their electron-poorer polar intermetallics generally adopt diverse extended structures with more delocalized bonding,[3] that is, as icosahedral and icosioctahedral clusters, so that the smaller numbers of valence electrons may be utilized. Particularly, these factors differentiate the roles of triels and tetrels in forming intermetallic clathrates: tetrels tend to define such host frameworks, whereas triels more often form clusters that act as guests within cationic frameworks. Electropositive metals (e.g., Na or Mg) that order as dodecahedral-like cages[4] often act in the latter roles.

Recently, intermetallic clathrates containing tetrels have been extensively explored, driven by their potential applications as thermoelectrics.[5] So far, there are about 110 intermetallic clathrate examples in the literature;[5c] ∼80% exhibit structural motifs of type I, ∼10% of type II, and the remaining exhibit types III, VIII, and IX (or better, c*P*124 clathrate for the last). However, no intermetallic examples of types IV−VII have been reported. (The classifications of clathrate types are in all cases defined by the geometries and packing of different cages.[5c,6]) Notably, most of these intermetallic clathrates are dominated by Si, Ge, or Sn elements, whereas only a few contain a major triel (Ga or In) component. Moreover, to date, the few clathrates that contain a major amount of a triel element evidently exhibit only type II clathrate structures.[4]

In principle, intermetallic clathrates containing triels should also be able to form other clathrate types. First, triels form

* To whom correspondence should be addressed. E-mail: jcorbett@iastate.edu

(1) Kauzlarich, S. M., Ed.; *Chemistry, Structure and Bonding of Zintl Phases and Ions*, VCH: New York, 1996.

(2) (a) Kröner, R.; Peters, K.; von Schnering, H. G.; Nesper, R. *Z. Kristallogr. NCS* **1998**, *213*, 664. (b) Zhao, J.-T.; Corbett, J. D. *Inorg. Chem.* **1994**, *33*, 5721. (c) Bobev, S.; Sevov, S. C. *J. Am. Chem. Soc.* **1999**, *121*, 3795. (d) Bobev, S.; Sevov, S. C. *Inorg. Chem.* **2000**, *39*, 5930. (e) Bobev, S.; Sevov, S. C. *J. Solid State Chem.* **2000**, *153*, 92. (f) Bobev, S.; Sevov, S. C. *J. Am. Chem. Soc.* **2001**, *123*, 3389. (g) Eisenmann, B.; Schäfer, H.; Zagler, R. *J. Less-Common Met.* **1986**, *118*, 43.

(3) Corbett, J. D. *Angew. Chem., Int. Ed.* **2000**, *39*, 670.

(4) (a) Li, B.; Corbett, J. D. *Inorg. Chem.* **2003**, *42*, 8768. (b) Li, B.; Corbett, J. D. *Inorg. Chem.* **2006**, *45*, 8958. (c) Lin, Q.; Corbett, J. D. *Inorg. Chem.* **2005**, *44*, 512. (d) Tillard-Charbonnel, M.; Belin, C. *Mater. Res. Bull.* **1992**, *27*, 1277. (e) Sevov, S. C.; Corbett, J. D. *Inorg. Chem.* **1993**, *32*, 1612.

(5) (a) Nolas, G. S.; Poon, J.; Kanatzidis, M. *MRS Bull.* **2006**, *31*, 199. (b) Nolas, G. S.; Slack, G. A.; Schujman, S. B. *Semiconduct. Semimet.* **2001**, *69*, 255. (c) Rogl, P. *Intl. Conf. Thermoelectrics* **2005**, *24th*, 443.

(6) Jeffrey, G. A. In *Inclusion Compounds*; Atwood, J. L., Davies, J. E. D., MacNicol, D. D., Eds.; Academic Press: London, 1984; pp 135−188.

10.1021/ic8003245 CCC: $40.75
Published on Web 10/29/2008

Table 1. Some Loaded Compositions, Reaction Conditions, and Products in the Li−Mg−Cu−Ga System and Lattice Parameters for the Title Phase

Li/Mg/Cu/Ga	condition[a]	phases in products or filtered products	lattice parameters (Å)[b]
10/3/6/21	A	>90% $(Li,Mg)_{13}Cu_6Ga_{21}$ (ref 7)	
9/4/6/21	A	>90% $(Li,Mg)_{13}Cu_6Ga_{21}$ (ref 7)	
7/6/6/21	A	60% $(Li,Mg)_{13}Cu_6Ga_{21}$ + 40% *P6m2*[c]	a = 14.110(2), c = 13.613 (3)
3/10/6/21	A	50% *P6m2* + 30%$Mg_{35}Cu_{24}Ga_{53}$+20%$(Li,Mg)_{13}Cu_6Ga_{21}$	a = 14.118 (1) c = 13.603 (2)
10/38.5/27.5/ 60	B	40% *P6m2* + 50% Mg_2Cu_3Ga + unknown	a = 14.111 (2) c = 13.626 (3)
10/48/21/60	B	40% *P6m2* + 60% MgGa	
7/28/10/55	C	75% *P6m2* + 25% $Mg_{35}Cu_{24}Ga_{53}$	a = 14.0951 (6), c = 13.5990 (7)
7/28/10/55	D	90% *P6m2* + 10% $Mg_{35}Cu_{24}Ga_{53}$	a = 14.0803 (4), c = 13.6252 (8)

[a] A: Heated to 800 °C at a rate of 60 °C/h, held for 5 days, then cooled to 400 °C at a rate of 5 °C/h and annealed at this temperature for 2 days. B: Heated to 700 °C at a rate of 120 °C/h, held for 2 h, cooled to 400 at 10 °C/h, and annealed at 400 °C for 2 days. C: Same as B, except that melts were cooled to 570 at 10 °C/h then 1 °C/h to 440 °C before rapid centrifugation and filtration at the last temperature. D: Same as C, except that sample was centrifuged and filtered at 480 °C. [b] From single-crystal data. [c] *P6m2* denotes the title phase.

polyhedral clusters that can be widely tuned, for example, in combinations with different late transition metals;[4b−d] second, the cationic cages may be stabilized by different-sized electropositive elements. In this work, we report the synthesis and structure of the first intermetallic exhibiting the acentric type IV clathrate structure, namely, $Li_{14.7(8)}Mg_{36.8(13)}Cu_{21.5(5)}Ga_{66}$, in which Li and most Mg define the host cages, whereas Cu and Ga form the anionic clusters, the guests. The discovery exemplifies a possible route to new clathrate structures and helps to define compositions for further searches for novel intermetallic clathrates.

Experimental Section

Syntheses. Appropriate amounts (∼400 mg) of Li foil (surface cleaned with a surgical blade), Mg turnings, Cu powder, and Ga chunks (all >99.9%, Alfa-Aesar) were weighed (±0.1 mg) in a helium-filled glovebox (H_2O <3.5 ppmv) and weld-sealed into small tantalum containers under an argon atmosphere. (Evaporation of Li or Mg was hereby avoided.) Then, containers were enclosed in evacuated SiO_2 jackets to avoid air oxidation during the high-temperature reaction process.

The title clathrate phase was first encountered after reactions of $Li_{13-x}Mg_xCu_6Ga_{21}$[7] compositions that were aimed at new Bergman-type quasicrystal and approximant phases through electronic tuning.[8] Table 1 lists the relevant reaction compositions and products. These samples were heated to 800 °C at a rate of 60 °C/h, held at this temperature for 5 days, then cooled to 400 °C at a rate of 10 °C/h, followed by annealing there for 2 days. After a preliminary single-crystal structural analysis, a stoichiometric reaction under the same conditions failed to give a high yield, only 40−50%. This is probably related to the particularly low melting point instead of gallium, which results in the physical segregation of liquid gallium, or an incongruent melting of the products, as often observed for gallium intermetallics.[4c,9]

Therefore, a self-fluxed method with filtration of crystalline products from excess liquid was applied by rapid centrifugation through a perforated Ta sieve after equilibration at a selected temperature, as also included in Table 1. This method has previously been successfully employed for other gallides, for example, $Mg_2Cu_6Ga_5$[10] and $Mg_{35}Cu_{24}Ga_{53}$.[4c] According to powder X-ray diffraction (XRD) analyses, the highest yields (∼90%) of the title phase were achieved by centrifugation of a nominal $Li_7Mg_{28}Cu_{10}Ga_{55}$ mixture. Before centrifugation, samples were first held at 700 °C for 2 h and then cooled to 570 °C at a rate of 10 °C/h and to 480 at 2 °C/h. The temperature for centrifugation is crucial for a good yield because a partial peritectoid decomposition to $Mg_{35}Cu_{24}Ga_{53}$[4c] and MgCuGa[11] and other unidentified phases evidently occurs at ∼475 °C on cooling according to thermal analyses (Figure S1, Supporting Information).

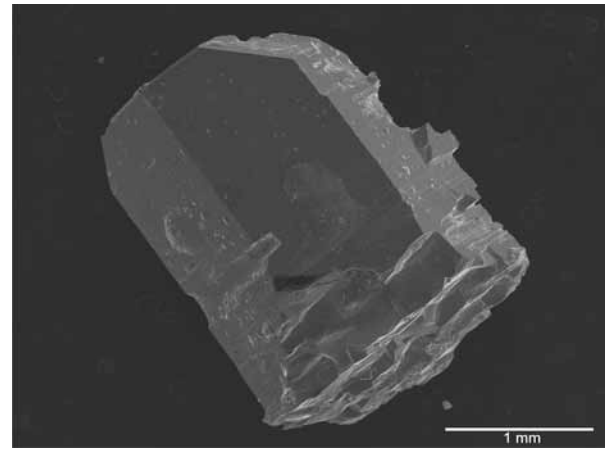

Figure 1. A typical SEM image of a $Li_{14.7}Mg_{36.8}Cu_{21.5}Ga_{66}$ crystal isolated by centrifugation with filtration. Note some melt residues on the crystal surfaces.

Intermetallics containing Li are sensitive to air and moisture, depending on the concentration, among other things. The present crystals turn black after one week's exposure to air at room temperature. So all reaction containers were opened in a crystal-mounting glovebox filled with dry N_2. Single crystals after filtration have well-formed hexagonal morphologies, Figure 1, and they are brittle and silvery with a metallic luster. The bulk crystals were crushed into small pieces. Some suitable crystals with clean surfaces, as guided by the eye with the help of a low-power microscope, were selected for single-crystal X-ray diffraction and inductively coupled plasma mass spectrometry (ICP-MS) analyses. According to lattice constants (Table 1), the title phase is not a line compound. However, no attempt has been made to establish the detailed homogeneity width of the phase.

ICP-MS Analyses. ICP-MS analyses were performed to establish the composition of the filtered product. Four single crystals with visually clean surfaces (under a low-power microscope), from the

(7) According to our LMTO-ASA calculations, the DOS of $Mg_{35}Cu_{24}Ga_{53}$[4c] exhibit a pseudogap (e/a = 2.20) just below the Fermi level (e/a = 2.26), whereas $Li_{13}Cu_6Ga_{21}$[20] shows a pseudogap (e/a = 2.18) just above the Fermi level (e/a = 2.05). These suggest that Li/Mg mixtures in both types might tune these phases to quasicrystals and approximant phases within a rigid band assumption.[8] In fact, the 1/1 Bergman phase with a range of composition of at least $Li_{8.6-10.3}Mg_{4.4-2.7}Cu_6Ga_{21}$ has been so obtained and characterized (Lin, Q.; Corbett, J. D. Unpublished results).

(8) Lin, Q.; Corbett, J. D. *Struct. Bonding (Berlin)*, **2008**, accepted.

(9) Belin, C.; Tillard-Charbonnel, M. *Prog. Solid State Chem.* **1993**, *22*, 59.

(10) Lin, Q.; Corbett, J. D. *Inorg. Chem.* **2003**, *42*, 8762.

(11) Mel'nik, E. V.; Kinzhibalo, V. V. *Izvest. Akad. Nauk SSSR, Met.* **1981**, 154.

Table 2. Crystal and Structural Refinement Data for $Li_{14.7}Mg_{36.8}Cu_{21.5}Ga_{66}$

formula	$Li_{14.7(8)}Mg_{36.8(13)}Cu_{21.5(5)}Ga_{66}$
normalized composition	$Li_{10.6(7)}Mg_{26.5(9)}$ $Cu_{15.4(4)}Ga_{47.5}$
ICP-MS composition	$Li_{11.9(9)}Mg_{23.6(5)}Cu_{15.6(2)}Ga_{48.9(5)}$
space group; Z	$P\bar{6}m2$; 1
unit cell	
a (Å)	14.0803(4)
c (Å)	13.6252(8)
V (Å^3)	2339.4(2)
fw (g/mol)/d_{cald} (mg/cm^3)	6963.7/4.9
abs coeff (mm^{-1})	23.6
ref coll./R_{int}	14829/0.0441
ref data/res./params	2175/0/133
GOF on F^2	1.104
R1/wR2 [$I > 2\sigma(I)$]	0.0647/0.1767
(all data)	0.0725/0.1864
max. residual peaks (e Å^3)	6.60 (1.48 Å from Cu2)/− 2.87

same batch as utilized for structural analyses, were separately dissolved in HNO_3 and diluted to the standard concentration range. Intensity data were calibrated according to an internal Sc standard. The average for the four measurements ($Li_{11.9(9)}Mg_{23.6(5)}$-$Cu_{15.6(2)}Ga_{48.9(5)}$) agrees with the normalized composition $Li_{10.6(7)}Mg_{26.5(9)}Cu_{15.4(4)}Ga_{47.5}$ refined from X-ray data to within 3σ.

Differential Thermal Analyses (DTA). Thermal analyses were performed under argon with the aid of a Perkin-Elmer Differential Thermal Analyzer (DTA-7). A ~20 mg sample was heated to 700 °C at a rate of 10 °C/min, then cooled to 300 °C at the same rate. A plot of the DTA output, together with enlarged XRD patterns measured at room temperature before and after the DTA scans, are given in Figure S1, Supporting Information.

X-Ray Studies. Phase identities were checked with the aid of a Huber 670 Guiner powder camera equipped with an imaging plate, monochromatic Cu Kα_1 radiation ($\lambda = 1.540598$ Å), and an internal standard of Si. Powdered samples were dispersed between pairs of Mylar sheets with the aid of petrolatum grease in a crystal glovebox (under a N_2 atmosphere). Data were collected under an operating voltage of 45 kV and a current of 20 mA, and a typical exposure time of 0.5 h. The detection limit of a second phase with this instrument and system is conservatively estimated to be about 5 vol % in equivalent scattering power.

For single-crystal structural studies, seven crystals from four different reactions were studied with a Bruker APEX CCD diffractometer equipped with graphite-monochromatized Mo Kα radiation. Intensity data were collected over a reciprocal space up to ~28° in θ and with exposures of 10−30 s per frame. Data integration, reduction, and standard corrections were made by means of the SAINT program.[12] Numeric absorption corrections were made by X-SHAPE.[13] Unit cell parameters were refined from all observed reflections [$I > 2\ \sigma(I)$]. Structural refinements for all crystals were performed with the aid of SHELXTL 6.1.[14] The refined compositions among these crystals were slightly different, but all structural refinements exhibited similar pathologies, as noted below. Therefore, the results for a crystal from the nominal $Li_7Mg_{28}Cu_{10}Ga_{55}$ synthetic composition for which ICP-MS analytical data were obtained are discussed here. Note that we also collected two STOE IPDS II data sets (3 and 5 min/frame), but no new and significant findings were obtained compared with the CCD results.

Systematic absence analyses all indicated primitive trigonal or hexagonal symmetries and the following candidate space groups: $P3$, $P\bar{3}$, $P321$, $P3m1$, $P\bar{3}m1$, $P312$, $P31m$, $P\bar{3}1m$, $P6$, $P\bar{6}$, $P\bar{6}m$, $P622$, $P6mm$, $P\bar{6}m2$, $P\bar{6}2m$, and $P6/mmm$. The space group with the highest symmetry ($P6/mmm$) was suggested by the SHELXTL program. Direct methods followed by difference Fourier syntheses yielded a model with 17 independent positions, and the final refinement with anisotropic displacements converged at R1 = 6.88% and wR2 = 16.98%, with a maximum residual peak of 6.75 e/Å^3. In this solution, one fractional Cu position with $mm2$ site symmetry was refined with ~55(1)% occupancy, generating a hexagonal ring ($6/m$ symmetry) with short separations (~1.51 Å) between neighboring equivalent neighbors (Figure S2, Supporting Information), which suggested a probably overestimated symmetry. Therefore, the lower symmetry space group $P3$ was temporarily assigned. This yielded, as expected, a model without any short bonds, but markedly high R values (R1 ~ 7.6%, wR2 ~ 23.2%) and abnormal U_{iso} values remained. Moreover, this solution did not pass examination by PLATON,[15] which indicated a higher symmetry space group, $P\bar{6}m2$. Nevertheless, other possible space groups (as listed above) were also tested, but none of them gave as reasonable a structural model as the following.

The initial direct-method solution in space group $P\bar{6}m2$ located 23 atoms, 16 with suitable separations for Cu/Ga pairs and seven for Mg−Cu/Ga pairs. Therefore, the first 16 positions were temporarily assigned as Ga and the remaining seven as Mg. After a few refinement cycles, the difference Fourier map yielded four more weakly scattering positions that were also temporarily assigned to Mg. Subsequent isotropic refinements converged at R1 ~ 11.6%. Checking of displacement parameters at this time revealed two abnormities: (1) Seven of the temporary Ga atoms had larger U_{iso} values (0.020−0.074 Å^2) compared with the average of the others (~ 0.015 Å^2), suggesting that they were either Cu or Cu/Mg (Cu/Li mixing in this system was considered unreasonable because Li has a distinctly smaller Mulliken electronegativity[16]). (2) Seven of 11 Mg positions had too large U_{iso} values (0.029−0.386 Å^2) compared with the average of the others (0.024 Å^2). Therefore, the two groups of problematic positions were respectively assigned to Cu and Li in subsequent refinements. At this time, four Cu's still had too large U_{iso} values (0.035−0.059 Å^2), and the U_{iso} values for six Li's went to extremes (0.0001 or 2.00 Å^2). So Cu/Mg and Mg/Li mixtures were assigned to the large "Cu" and "Li" positions in following refinements. However, large U_{iso} values remained for four Mg/Li positions after refinements, suggesting that these four were pure Li. Also, U_{iso} values of the three of these that center anionic polyhedra (below) remained at 0.0001 Å^2 after a few cycles of refinements. In later refinements, the displacement parameters for all four Li atoms were fixed at 0.038 Å^2, which was about the U_{iso} of the more normal Li2 in previous refinement cycles, 0.0375 Å^2. These treatments led to a slightly lower isotropic refinement index, R1 ~ 10.0%. Noteworthily, attempts to refine Cu/Ga mixtures resulted in either divergent or unstable refinements, the same as previously encountered,[4c,10] likely because of their very similar electron counts or their distinctively different structural roles in polyhedral construction in general.

The final least-squares refinements, with anisotropic displacement parameters, converged at R1 = 6.47%, wR2 = 17.67%, and GOF = 1.104, with 133 parameters refined from 2175 independent reflections. At this stage, no higher symmetry was indicated after rechecking with PLATON.[4] The refined composition, $Li_{14.7(8)}$-$Mg_{36.8(13)}Cu_{21.5(5)}Ga_{66}$, or that normalized in percentages,

(12) *SMART*; Bruker AXS, Inc.: Madison, WI, 1996.
(13) *STOE WinXPOW, STOE & Cie Gmbh*, v 2.10; Hilpertst: Darmstadt, Germany, 2004.
(14) *SHELXTL*; Bruker AXS, Inc, Madison, WI, 1997.
(15) Spek, A. L. *J. Appl. Crystallogr.* **2003**, *36*, 7.
(16) Pearson, R. G. *Inorg. Chem.* **1988**, *27*, 734.

Table 3. Atomic Coordinates and Equivalent Isotropic Displacement Parameters (Å^2) for $Li_{14.7}Mg_{36.8}Cu_{21.5}Ga_{66}$

atom	Wyck.	symm.	*x*	*y*	*z*	*U*(eq) (Å^2)[a]	occ. ≠ 1
Ga1	12*o*	1	0.0002(2)	0.1887(1)	0.18700(9)	0.014(1)	
Ga2	12*o*	1	0.0003(2)	0.3441(1)	0.0995(1)	0.016(1)	
Ga3	6*n*	.m.	0.2238(2)	−*x*	0.4037(3)	0.032(1)	
Ga4	6*n*	.m.	0.3968(1)	−*x*	0.3160(2)	0.018(1)	
Ga5	6*n*	.m.	0.4493(1)	−*x*	0.1595(2)	0.015(1)	
Ga6	6*n*	.m.	0.5516(1)	−*x*	0.1590(2)	0.016(1)	
Ga7	6*n*	.m.	0.6027 (1)	−*x*	0.3150(3)	0.022(1)	
Ga8	6*l*	m..	0.1568(2)	0.4870(2)	0	0.014(1)	
Ga9	6*l*	m..	0.4879(2)	0.1567(2)	0	0.013(1)	
Cu1	6*n*	.m.	0.7767(2)	−*x*	0.4051(3)	0.039(1)	
Cu2	3*k*	mm2	0.0614(2)	−*x*	1/2	0.022(1)	
Cu3	3*k*	mm2	0.4465(3)	−*x*	1/2	0.182(9)	
Cu/Mg1	6*n*	.m.	0.1226(2)	−*x*	0.3475(4)	0.027(2)	0.75/0.25(3)
Cu/Mg2	6*n*	.m.	0.8788(2)	−*x*	0.3517(5)	0.026(2)	0.43/0.57(3)
Cu/Mg3	3*k*	mm2	0.5522(3)	−*x*	1/2	0.026(3)	0.40/0.60(3)
Cu/Mg4	2*g*	3m.	0	0	0.0947(4)	0.027(2)	0.62/0. 38(3)
Mg1	3*j*	mm2	0.1288(6)	−*x*	0	0.029(3)	
Mg2	3*j*	mm2	0.8658(6)	−*x*	0	0.029(5)	
Mg3	2*h*	3m.	1/3	2/3	0.124(1)	0.020(3)	
Mg4	6*n*	.m.	0.7910(4)	−*x*	0.1909(6)	0.023(3)	
Mg/Li1	12*o*	1	0.3772(6)	−0.0001(8)	0.3076(4)	0.022(2)	0.78/0.22(3)
Mg/Li2	6*m*	m..	0.3096(9)	0.0498(11)	1/2	0.035(4)	0.80/0.20(5)
Mg/Li3	2*i*	3m.	2/3	1/3	0.120(2)	0.020(2)	0.52 /0.48(6)
Li1	6*n*	.m.	0.212(3)	0.424(5)	0.191(6)	0.038[b]	
Li2	2*g*	3m.	0	0	0.292(6)	0.038[b]	
Li3	1*f*	−6m2	2/3	1/3	1/2	0.038[b]	
Li4	1*d*	−6m2	1/3	2/3	1/2	0.038[b]	

[a] *U*(eq) is defined as one-third of the trace of the orthogonalized u^{ij} tensor. [b] Fixed *U*(eq).

Table 4. Selected Inter- and Intracluster Bond Distances in the Anionic Network in $Li_{14.7}Mg_{36.8}Cu_{21.5}Ga_{66}$

bond[a]	dist. (Å)[b]	bond	dist. (Å)	bond	dist. (Å)	bond	dist. (Å)
Ga1−Ga2	**2.491(3)**	Ga1−Ga1	2.651(3)	Ga3−Ga3	2.624(6)	Ga7−M3	2.806(4)
Ga3−M1	**2.584(4)**	Ga1−Ga1	2.659(2)	Ga3−Ga4	2.612(3)	Ga8−Ga8	2.574(3)
Ga4−Ga5	**2.487(4)**	Ga1−M2	2.690(6)	Ga3−Cu3	3.017(4)	Ga9−Ga6	2.597(3)
Ga6−Ga7	**2.465(5)**	Ga1−M1	2.649(5)	Ga4−Ga4	2.680(2)	Ga9−Ga9	2.547(3)
Ga8−Ga8	**2.442(3)**	Ga1−M4	2.938(3)	Ga4−Cu3	2.785(3)	Cu1−Cu1	2.586(6)
Ga9−Ga9	**2.457(3)**	Ga2−Ga2	2.711(2)	Ga5−Ga6	2.494(3)	Cu1−M3	3.029(4)
Cu1−M2	**2.594(5)**	Ga2−Ga5	2.650(2)	Ga5−Ga8	2.614(2)	Cu2−Cu2	2.595(3)
Cu3−M3	**2.578(7)**	Ga2−Ga6	2.660(3)	Ga6−Ga9	2.597(2)	Cu2−M1	2.558(5)
M4−M4	**2.581(8)**	Ga2−Ga8	2.512(2)	Ga7−Ga7	2.700(2)	M1−M2	2.974(3)
		Ga2−Ga9	2.521(4)	Ga7−Cu1	2.638(3)		

[a] M represents Cu/Mg mixtures. [b] Bold data represent intercluster distances.

$Li_{10.6(7)}Mg_{26.5(9)}Cu_{15.4(4)}Ga_{47.5}$, agrees reasonably with the ICP-MS result, $Li_{11.9(9)}Mg_{23.6(5)}Cu_{15.6(2)}Ga_{48.9(5)}$. (The difference in Mg contents is 3σ.)

The residual peaks in the final difference Fourier map are somewhat high considering the presence of Li, even Mg, in the system. The three largest are 6.6 *e*/Å^3 (1.48 Å from Cu2), 6.5 *e*/Å^3 (1.52 Å from Cu/Mg3), and 5.2 *e*/Å^3 (1.58 Å from Cu3). However, these probably are not real atoms because (1) the distances to normal atoms are unreasonably small; (2) the next highest residuals decrease gradually *not* abruptly, that is, the fourth strongest peak is ∼ 4.1 *e*/Å^3, the fifth is 2.5 *e*/Å^3, and the sixth is 2.1 *e*/Å^3; (3) these residuals correlate strongly with the weakest observed reflections in the resolution range from ∼1.7 Å to infinity, which is normal for structures with light elements that exhibit positional disorders. A parallel refinement omitting these low-resolution reflections (>1.7 Å) greatly decreases residual peaks (3.39 *e*/Å^3 and −1.91 *e*/Å^3) and converges at R1 = 5.39%, wR2 = 13.02%, and GOF = 1.087 for 1958 reflections. Another imperfection is that Cu3 refines with an elongated cigarlike ellipsoid, which normally suggests split positions in crystallography. It was refined with an atom at its center instead because such an abnormal ellipsoid results from not only a positional disorder, but also from the distortions of the M_{24} cage (see Figure S3, Supporting Information).

Nevertheless, both pathologies, the somewhat high residuals and some disorder, seem to be intrinsic to this structure, as they also appeared in structural solutions with both *P*6/*mmm* (Figure S2, Supporting Information) and *P*3 space groups, and however the reaction compositions and conditions were varied (above). That is, the problems were persistent with all seven crystals from four different reactions that we analyzed, and regardless of the different diffractometers used.

Table 2 summarizes the crystal and structural refinement; Table 3 lists the refined positional parameters, standardized with TIDY,[17] and Table 4 lists the important interatomic distances within the extended 3D Cu/Ga anionic framework. The remaining crystallographic data are given in a CIF file in the Supporting Information.

Electronic Structure Calculations. The electronic structure of the title phase, $Li_{15.5(11)}Mg_{36.0(16)}Cu_{21.5(5)}Ga_{66}$, was approximated by a calculation on the idealized anionic framework $[Cu_{29}Ga_{66}]^{73-}$ with the aid of *CAESAR*,[18] a semiempirical EHTB program. This formula was obtained by assuming that all sites with mixed Cu/Mg occupancies (40−70% Cu) were fully occupied by Cu, whereas the net charge was derived according to a classic electron-counting

(17) Gelato, L. M.; Parthé, E. *J. Appl. Crystallogr.* **1987**, *20*, 139.
(18) Ren, J.; Liang, W.; Whangbo, M.-H. *CAESAR for Windows*; Prime-Color Software Inc., North Carolina State University: Raleigh, NC, 1998.

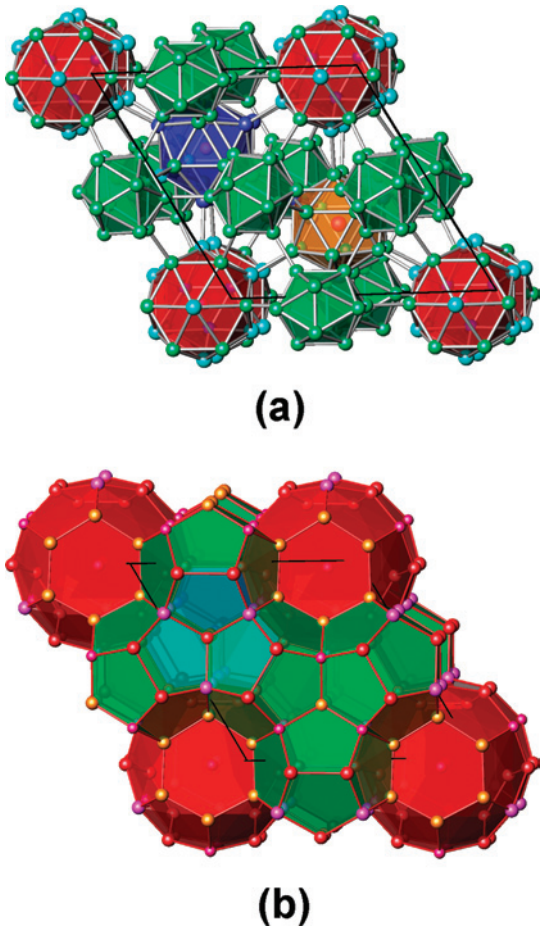

Figure 2. ~[001] projections of the three-dimensional frameworks of (a) interbonded anionic (Cu/Ga) polyhedral clusters and (b) cationic (Li/Mg) cages in $Li_{14.7}Mg_{36.8}Cu_{21.5}Ga_{66}$. Condensation of M_{20} (green), M_{24} (red), and M_{26} (blue and orange) cages in b mimic the typical configuration of type IV clathrates. A detailed color scheme is given in Figure 3.

scheme (below). The following orbital energies and exponents were employed in the calculation (H_{ii} = orbital energy (eV), ξ = Slater exponent). Cu: 3d, $H_{ii} = -14.0$, $\xi = 5.95$, c1 = 0.5933, $\xi_{22} = 2.30$, c2 = 0.5744; 4s, $H_{ii} = -11.40$, $\xi = 2.2$; 4p, $H_{ii} = -6.06$, $\xi = 2.2$. Ga: 4s, $H_{ii} = -14.58$, $\xi = 1.77$; 4p, $H_{ii} = -6.75$, $\xi = 1.55$.[19]

Results and Discussion

Structural Description. The phase $Li_{14.7(8)}Mg_{36.8(13)}Cu_{21.5(5)}Ga_{66}$ represents a new structural type (*h*P139, $P\bar{6}m2$, $Z = 1$). According to the lattice parameters ($a \approx 14.08$ Å, $c \approx 13.63$ Å), the title phase can be viewed as an augmented and distorted version of the cubic $Li_{13}Cu_6Ga_{21}$[20] ($Im\bar{3}$, $a = 13.57$ Å) phase that is driven by the substitution of some Li by Mg. Actually, when the Mg content is small, that is, $x \leq 4$ in $Li_{13-x}Mg_xCu_6Ga_{21}$ (Table 1), the products are dominated by the same cubic phase (>90% yield) with $a \approx 13.63$ Å.[7] Therefore, it is not surprising that the present hexagonal structure also contains the four-shell 104-atom Bergman clusters that exist in the parent $Li_{13}Cu_6Ga_{21}$.[20] However, such a description is not customary or favored here because the Bergman-type clusters cut each other in the primitive hexagonal packing. Moreover, this approach would leave some important structural features unaccounted for, as below.

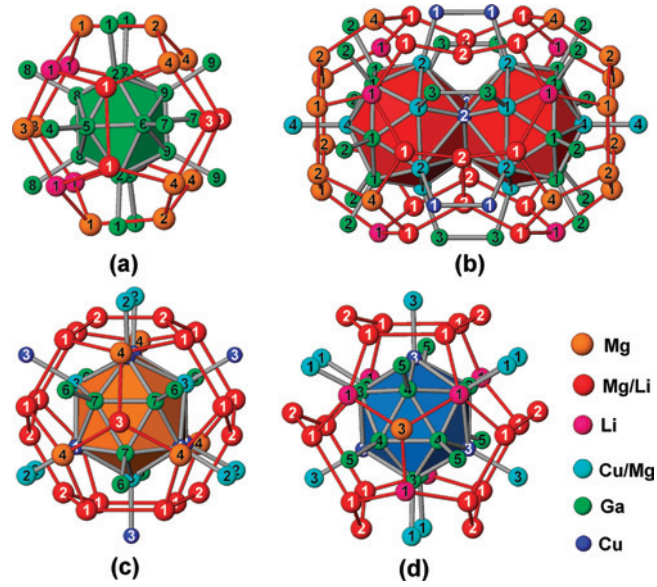

Figure 3. The anionic polyhedral clusters enclosed in differently sized cation cages in $Li_{14.7}Mg_{36.8}Cu_{21.5}Ga_{66}$. (a) The Ga_{12} icosahedron (green) in an M_{20} cage, (b) a pair of confacial $Li@(Cu,Mg)_{10}Ga_6$ icosioctahedra (red) in two condensed M_{24} cages ($\approx M_{42}$), (c) the $Li@(Cu,Mg)_9Ga_6$ polyhedron (orange) in an M_{26} cage, and (d) the $Li@Cu_3Ga_{12}$ (blue) in another M_{26} cage. The exobonds of each anionic cluster are shown. Numbers mark atomic labels given in Table 3 except that Li2−Li4 cluster-centering atoms are not shown.

Figure 2 shows the three-dimensional polyhedral frameworks of the anions in panel a and the cations in panel b. The two frameworks intermesh in such a way that the anionic polyhedra are encapsulated within the cationic cages, as is customary. The absence of an inversion center is evident judging from each framework at the unit cell level.

The cationic framework consists of three different types of cages: M_{20} (or 5^{12}), M_{24} ($5^{12}6^2$), and M_{26} ($5^{12}6^3$) (M = Mg, Mg/Li, Li), in which the notation in parentheses denotes the number of pentagonal and hexagonal faces for each polyhedron, whereas the subscripts of M key the number of vertices of each polyhedron. The ratio of the three cage types is $M_{20}/M_{24}/M_{26} = 3:2:2$. Viewed along the *c* direction, Figure 2b, layers of the face-sharing M_{20} cages (green) and M_{26} cages (orange and blue), both with hexagonal packing, alternate with layers of M_{24} cages (red), also hexagonally packed, at $z = 0$ and 1/2, respectively. Noteworthily, the geometries, the packing, and the proportions among these cationic cages follow the classification of a type IV clathrate. An *ideal* type IV clathrate, extrapolated from known clathrate hydrates, would be expected to exhibit *P*6/*mmm* symmetry, and to contain six M_{20}, four M_{24}, and four M_{26} face-sharing host cages in a unit cell.[5c,6] However, no such type IV structure has been experimentally established before, although two lower-symmetry hydrate versions[21] and two clathrate-related organometallic examples[22] are available. The structure of $Li_{38}(Ga_{0.666}Zn_{0.333})_{101}$,[23] *P*6/*mmm*, also seems to

(19) Tillard-Charbonnel, M.; Belin, C. *Inorg. Chem.* **2000**, *39*, 1684.
(20) Tillard-Charbonnel, M.; Belin, C. *J. Solid State Chem.* **1991**, *90*, 270.
(21) (a) Feil, D.; Jeffrey, G. A. *J. Chem. Phys.* **1961**, *35*, 1863. (b) Beurskens, P. T.; Jeffrey, G. A. *J. Chem. Phys.* **1964**, *40*, 2800.
(22) Wiebcke, M.; Mootz, D. *Z. Kristallogr.* **1988**, *183*, 1.

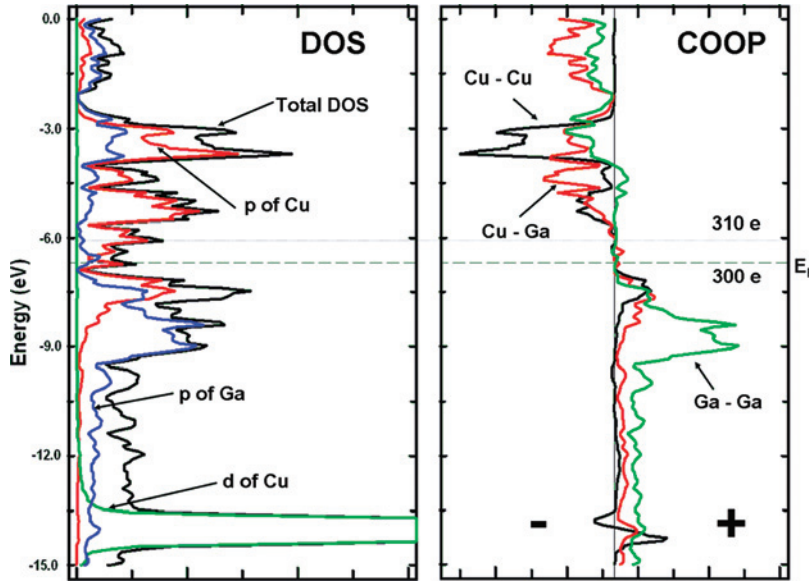

Figure 4. DOS and COOP data for the "$[Cu_{29}Ga_{66}]^{73-}$" model of $Li_{14.7}Mg_{36.8}Cu_{21.5}Ga_{66}$, showing that bonding in this cation-free model is substantially optimized.

exhibit structural motifs of a type IV clathrate; however, it is somewhat unlikely that the reported cationic cages are built of electronegative atoms as well, and that the anionic polymetal clusters in M_{26} cages are 16-vertex, not the 15-vertex polyhedra observed here (below).

Figure 3 shows the detailed host−guest relationships between the four cationic cages and anionic polyhedral clusters. In the present structure, (a) each M_{20} cage encloses a Ga_{12} icosahedron, (b) each M_{24} cage contains a Li2-centered $(Cu,Mg)_{10}Ga_6$ icosioctahedron, and each M_{26} cage encloses either (c) a Li3-centered $(Cu,Mg)_9Ga_6$ polyhedron or (d) a Li4-centered Cu_3Ga_{12} polyhedron in an ordered way. The anionic polyhedral clusters are guests in the electropositive metal cages, in contrast to heteromolecules found within hydrogen-bonded water cages in hydrate clathrates.[6] In addition, the present anionic polyhedra are also interconnected by presumed two-center−two-electron (2c−2e) bonds between all Cu, Cu/Mg, or Ga vertices, except that two neighboring Li2-centered $(Cu,Mg)_{10}Ga_6$ icosioctahedra share a Cu_3 triangular face to generate a dimeric unit, $Li_2@(Cu,Mg)_{17}Ga_{12}$ (Figure 3b). As before,[4c] the intercluster distances (2.44−2.59 Å) are generally shorter than the intracluster bond distances (2.51−3.03 Å), Table 4, suggesting more typically electron-poorer and delocalized bonding within the clusters. The separations between electropositive M atoms fall within the range of 2.93−3.35 Å, M = Mg, Li, Mg/Li, close to those within $Li_{13}Cu_6Ga_{21}$ (2.94−3.15 Å)[20] and $Mg_{35}Cu_{24}Ga_{53}$ (3.15−3.24 Å).[4c] These are, of course, largely determined by packing.

Nature always orders reasonably. The preference of the largest $Li@(Cu,Mg)_{10}Ga_6$ icosioctahedon for the medium-sized M_{24} cage rather than the M_{26} version is delicately avoided by one further degree of condensation, that is, to these cluster dimers. Each cluster shares a Cu_3 triangular face with a like neighboring cluster, accompanied by the elimination of one-half of the Mg/Li2−Mg/Li2 bonds on the shared hexagonal faces between M_{24} cages (Figure 3b). Such mutual compensations follow both crystallographic and bonding requirements, the latter being discussed below.

Electron and Bonding Requirements. Some classic electron counting rules for the polyanions are apparently applicable in the present structure because of the host−guest relationships between cationic cages and anionic polyhedral clusters. Normally, stabilization of an isolated icosahedron requires 26 skeletal electrons according to Wade's rules,[24] and the closo 15-vertex polyhedron needs 32 skeletal electrons according to King.[25] As for the closo 16-vertex icosioctahedron, earlier extended-Hückel calculations revealed that 36 skeletal electrons are optimal.[4c] In the present structure, however, the last value is not applicable because a pair of icosioctahedra share a triangle face, so the dimeric unit $Li_2@(Cu,Mg)_{17}Ga_{12}$ should be considered. Again, extended Hückel calculations by Mingos[26] have shown that 66 skeletal electrons are the most reasonable count for this 29-atom dimer unit. Because all anionic polyhedra are interconnected by 2c−2e bonds, each Ga_{12} icosahedron also requires 12 exobonding electrons, the $Li_2@(Cu,Mg)_{17}Ga_{12}$ dimer unit should need 26 more (the three Cu atoms on the shared face do not have exo bonds, see Figure 3b), and each 15-vertex polyhedron needs 15 exobonding electrons. Each unit cell contains three Ga_{12} icosahedra, one $Li_2@(Cu,Mg)_{17}Ga_{12}$ dimer unit, and two 15-vertex polyhedra. Therefore, stabilization of the anionic framework requires a total of $(26 + 12) \times 3 + (66 + 26) \times 1 + (32 + 15) \times 2 = 300$ electrons ($Z = 1$). This value agrees within 2σ with the valence electron sum provided by all constituent elements, 307.8 ± 3.9. The electron counting scheme is summarized in Table 5. The large deviation comes mainly from the

(23) Tillard-Charbonnel, M.; Chouaibi, N.; Belin, C.; Lapasset, J. *Eur. J. Solid State Inorg. Chem* **1992**, *29*, 347.

(24) Wade, K. *Adv. Inorg. Chem. Radiochem.* **1976**, *18*, 1.
(25) King, R. B. *J. Organomet. Chem.* **2007**, *692*, 1773.
(26) Mingos, D. M. P. *Acc. Chem. Res.* **1987**, *17*, 311.

Table 5. Classical Electron Counting Scheme for $Li_{14.7}Mg_{36.8}Cu_{21.5}Ga_{66}$

	Ga_{12}	Li_2@ $(Cu,Mg)_{17}$ Ga_{12}	Li@Cu_3 Ga_{12}	Li@ $(Cu,Mg)_9$ Ga_6
skeleton electrons/ cluster	26	66	32	32
exobonding electrons/ cluster	12	26	15	15
multiplicity	3	1	1	1
electron required	114	92	47	47
total electrons required/cell	300			
total electrons from refined composition/cell	307.8 ± 3.9			
difference/cell	7.8 ± 3.9			

uncertainties of refined Li/Mg and Mg/Cu mixtures, and a decrease in the Mg proportion following the analytical data would lower the number. Nevertheless, the present phase is not a line compound according to lattice constants (Table 1), and the electronic structural calculation suggests that this structure is stable near this electron count (below).

Figure 4 shows the density-of-states (DOS) and crystal orbital overlap population (COOP) for this anion framework. Judging from the DOS curves, this new phase would be metallic. As usual, the Cu 3d orbitals are low, in the −13.5 to −15.0 eV energy range, and not very involved in bonding, whereas mainly Cu and Ga 4p orbitals generate states around the Fermi energy. From the COOP data, the highest-lying bonding states falling in the energy range between E_F ∼−6.68 eV and −6.08 eV, which correspond to 300 and 310 electrons per cell, respectively, are optimized (excluding Cu $3d^{10}$).

Of course, both electron counting and EHTB calculation assessments assume that the electrons are localized in the observed clusters and that the phase is not significantly metallic. Recall however that all anionic clusters are directly interbonded (Figure 2a) and this would favor intercluster communication and lead to interactions on a larger scale, that is, delocalization.

Conclusions

In summary, an intermetallic exhibiting the characteristic type IV clathrate structural pattern is now available. The structure features hexagonal packing of face-sharing M_{20} (5^{12}), M_{24} ($5^{12}6^2$), and M_{26} ($5^{12}6^3$) cages, inside of which anionic polyhedral clusters of Ga_{12} icosahedra, 16-vertex icosioctahedra Li@$(Cu,Mg)_{10}Ga_6$, and 15-vertex Li@$(Cu,Mg)_9Ga_6$ and Li@Cu_3Ga_{12} polyhedra are hosted, respectively. In this structure, the functionalities for Li/Mg versus Cu/Ga pairs are markedly different, and all host cages are complete, in contrast to its hydrate relatives.[21] The unique structural motif possibly comes from the distinctive roles played by Cu and Ga in the anionic clusters, as observed before,[4c,10] and by Li and Mg within the cationic cages as well. Some intrinsic disorder is also evident. Discovery of the title phase calls for further consideration of this rare clathrate type and may shed new light on the future design of other clathrates.

Acknowledgment. The authors thank R. S. Houk for allowing use of the equipment, N. Saetveit for collection and analyses of the ICP-MS data, and K. Dennis for use of the DTA instruments. This research was supported by the U.S. National Science Foundation, Solid State Chemistry, via grant DMR-0444657 and was performed in the facilities of the Ames Laboratory, U.S. Department of Energy.

Supporting Information Available: Detailed crystallographic data in CIF format and Figures S1−S3 with DTA and further structural interpretations are deposited. These materials are available free of charge via the Internet at http://pubs.acs.org.

IC8003245